I-5 COMPUTER SOLUTION OF WAVE-GUIDE DISCONTINUITY PROBLEMS

P.J.B. Clarricoats

Leeds University, England

K.R. Slinn

Microwave Associates, Inc.

A technique has been developed which enables two important classes of wave-guide discontinuity problem to be solved on a computer by simple numerical methods. The classes are:

1. Transverse discontinuities.
2. Longitudinal discontinuities.

Examples of the first class are (i) a step-change in waveguide cross-section where the step lies entirely in a plane transverse to the direction of propagation; (ii) a step-change in the cross-section of a dielectric contained within a homogeneous waveguide as in Fig. 1.; (iii) a combination of (i) and (ii); (iv) discontinuities of finite thickness made up from two steps of kinds (i) or (ii) as in Fig. 2(a). In the above cases, our method enables the complex reflection and complex transmission coefficient of the propagating modes to be determined with high accuracy; the method is, in principle, unrestricted in the number of propagating modes. In simple cases we have obtained the equivalent circuit parameters and have made favourable comparison with values obtained by analytic and experimental methods. An example belonging to the second class is provided by a waveguide of uniform cross-section containing a slot of uniform width in a waveguide wall of finite thickness, as in Fig. 3. The slot discontinuity thus lies in a longitudinal plane with respect to the direction of propagation. In this case, the method enables the complex propagation coefficient of the leaky-waveguide modes to be determined without restriction on the slot width. We have applied the method to the case of a slotted circular waveguide and have obtained results which agree precisely with experiment. Another example belonging to the second class is provided by the coupled waveguide of Fig. 4.

A description of the method, as applied to class 1, has been given previously by the authors [1] and the results shown in Figures 1 and 2 provide an indication of the accuracy which may be obtained. The extension of the method to the second class of problem follows rather closely that for the thick iris and, in the interest of brevity, in this abstract only this case will be described in outline form.

Fig. 2(b) shows a general schematic equivalent circuit representation for the thick inductive iris of Fig. 2(a). If $\underline{E}_t$ and $\underline{H}_t$ are the transverse electric and transverse magnetic fields in the waveguide respectively, then the boundary conditions over the aperture at A and B lead to equations (1) through (4).

$$(1+\tau_1')E_{t1} + \sum_2^{\infty} \tau_n' E_{tn} = \sum_1^{\infty} \tau_N E_{tN} + \sum_1^{\infty} \tau_N' E_{tN} \qquad (1)$$

$$(1-\tau_1')H_{t1} - \sum_2^{\infty} \tau_n' H_{tn} = \sum_1^{\infty} \tau_N H_{tN} - \sum_1^{\infty} \tau_N' H_{tN} \qquad (2)$$

$$\sum_1^{\infty} \tau_N E_{tN} e^{-\gamma_N \ell} + \sum_1^{\infty} \tau_N' E_{tN} e^{\gamma_N \ell} = \sum_1^{\infty} \tau_n E_{tn} \qquad (3)$$

$$\sum_1^{\infty} \tau_N H_{tN} e^{-\gamma_N \ell} - \sum_1^{\infty} \tau_N' H_{tN} e^{\gamma_N \ell} = \sum_1^{\infty} \tau_n H_{tn} \qquad (4)$$

We now transform the equations to a form suitable for numerical analysis. Vector post-multiply equation (1) by $\underline{H}_{t_m}^*$ and integrate over the aperture. By using the boundary condition that the left-hand side of equation (1) is zero over the iris and, on utilizing the well-known orthogonality relation, we obtain equation (5).

$$\tau_m' \int_s \underline{E}_{t_m} \times \underline{H}_{t_m}^* \cdot \underline{ds} - \sum_1^{\infty} (\tau_N + \tau_N') \int_{ap} \underline{E}_{tN} \times \underline{H}_{t_m}^* \cdot \underline{ds} = -\delta_{m1} \int_s \underline{E}_{t1} \times \underline{H}_{t1}^* \cdot ds \qquad (5)$$

$$m = 1, 2, \ldots \infty$$

Vector pre-multiply the conjugate of equation (2) by $\underline{E}_{t_M}$ integrate over the aperture and use orthogonality on the right-hand side of the equation.

$$\sum_1^{\infty} \tau_n'^* \int_{ap} \underline{E}_{t_M} \times \underline{H}_{t_n}^* \cdot \underline{ds} + (\tau_M^* - \tau_M'^*) \int_{ap} \underline{E}_{t_M} \times \underline{H}_{t_M} \cdot \underline{ds} = \int_{ap} \underline{E}_{t_M} \times \underline{H}_{t_1}^* \cdot \underline{ds} \qquad (6)$$

$$M = 1, 2, \ldots \infty$$

Equations (3) and (4) are similarly modified to give equations (7) and (8).

$$\sum_1^{\infty} (\tau_N e^{-\gamma_N \ell} + \tau_N' e^{\gamma_N \ell}) \int_{ap} \underline{E}_{tN} \times \underline{H}_{t_m}^* \cdot ds - \tau_m \int_s \underline{E}_{tm} \times \overline{\underline{H}_{t_m}^*} \cdot \underline{ds} = 0 \qquad (7)$$

$$(\tau_M^* e^{-\gamma_{N^*} \ell} - \tau_M'^* e^{\gamma_{N^*} \ell}) \int_{ap} \underline{E}_{tM} \times \underline{H}_{t_M}^* \cdot \underline{ds} - \sum_1^{\infty} \tau_n^* \int_{ap} \underline{E}_{t_M} \times \underline{H}_{t_n}^* \cdot \underline{ds} = 0 \qquad (8)$$

$$M = 1, 2, \ldots \infty$$

In our method the infinite series are terminated after a finite number of terms yielding four finite sets of equations which may be solved simultaneously, to obtain the reflection and transmission coefficients for the iris. It is not necessary, incidentally, to choose the same number of terms in each series.

We have performed calculations for an iris of thickness $\ell/a = 0.035$ with $a/\lambda_0 = 0.8$. Seven modes are used in each region and the error compared with the final extrapolated value, over the range $0.2 < d/a < 0.8$, is less than 1%. Comparison with results obtained by other authors is shown in Fig. 2(a).

The analysis of a longitudinal discontinuity such as that depicted in Fig. 3, proceeds in a manner similar to the thick iris. If a transverse modal representation is chosen, following Goldstone and Oliner[(2)] application of boundary conditions at $r = r_o$ and $r = r_o + \ell$ and use of orthogonality conditions, leads to the four equations given below.

$$V_m^{(1)}(r_o) - \sum_o^{\infty} V_n^{(2)}(r_o) \int_{-\phi_o}^{\phi_o} \underline{e}_{t_n}^{(2)} \times \underline{h}_{t_m}^{(1)}(r_o)\underline{i}_r \, r d\theta = 0. \quad m = 0, 1 \ldots \infty \tag{9}$$

$$\sum_o^{\infty} I_n^{(1)}(r_o) \int_{-\phi_o}^{\phi_o} \underline{e}_{t_m}^{(2)} \times \underline{h}_{t_n}^{(1)}(r_o) \cdot \underline{i}_r \, r d\theta - I_m^{(2)}(r_o) = 0. \quad m = 0, 1 \ldots \infty \tag{10}$$

$$\sum_o^{\infty} V_n^{(2)}(r_o + \ell) \int_{-\phi_o}^{\phi_o} \underline{e}_{t_n}^{(2)} \times \underline{h}_{t_m}^{(3)}(r_o + \ell) \cdot \underline{i}_r \, r d\theta - V_m^{(3)}(r_o + \ell) = 0 \quad m = 0, 1 \ldots \infty \tag{11}$$

$$I_m^{(2)}(r_o + \ell) - \sum_o^{\infty} I_n^{(3)}(r_o + \ell) \int_{-\phi_o}^{\phi_o} \underline{e}_{t_m}^{(2)} \times \underline{h}_{t_n}^{(3)}(r_o + \ell) \cdot \underline{i}_r \, r d\theta = 0 \quad m = 0, 1 \ldots \infty \tag{12}$$

As before, the series are truncated after a finite number of terms. The modal terms $V_m^{(1)}(r_o)$, etc., comprise a complex coefficient and a complex function, dependent upon the complex propagation coefficient. When appropriate substitutions are made for these functions, a system of simultaneous equations result and, if M modes are included in each region, 8 x M equations result. The condition that the determinant of these equations shall vanish provides a means for evaluating the complex propagation coefficient. This has been done for the case of a circular waveguide supporting an H_{11} leaky waveguide mode. The number of modes taken in each region does not have to be the same and, in our evaluation, 9 modes were chosen in the inner and outer regions and 3 in the slot. Fig. 3. shows the normalized phase-change coefficient and normalized attenuation coefficient as a function of normalized waveguide radius. The results are compared with the experimental results of Goldstone and Oliner[2] and their theoretical results, obtained by use of perturbation and small aperture formulae.

The extension of this technique to other microwave discontinuity problems is under consideration. Taken in conjunction with finite-difference methods, problems such as the step-discontinuity between two waveguides of arbitrary cross-section should be amenable to solution.

1. CLARRICOATS, P.J.B. and SLINN, K.R.: 'Numerical method for the solution of waveguide-discontinuity problems', Electronics Letters, June 1966, Vol. 2, No. 6, p.226.
2. GOLDSTONE, L.O. and OLINER, A.A.: 'Leaky wave antennas', I.R.E. Trans. on Antennas and Propagation, Pt. 1 (Rectangular waveguides), 1959, AP-7, p.307, Pt. II (Circular waveguides), 1961, AP-9, p.280.

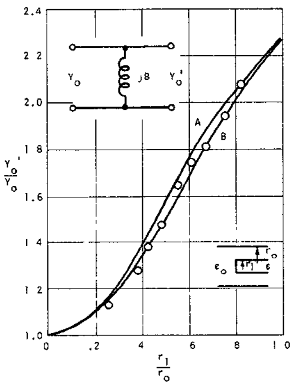

CURVE A β'/β = PHASE-CHANGE COEFFICIENT OF TE_{11} MODE IN HOMOGENEOUS WAVEGUIDE
β' = PHASE-CHANGE COEFFICIENT OF TE_{11}-TYPE MODE IN HOMOGENEOUS WAVEGUIDE
CURVE B Y_o'/Y_o FROM NUMERICAL SOLUTION EMPLOYING 3 MODES IN EACH WAVEGUIDE

DATA. $\frac{2\pi r_o}{\lambda_o}$ = 2 322, $\frac{\epsilon}{\epsilon_o}$ = 2 56 EXPERIMENTAL RESULTS ARE DUE TO McBRIDE

Figure 1 (a) Network parameters for dielectric rod junction.

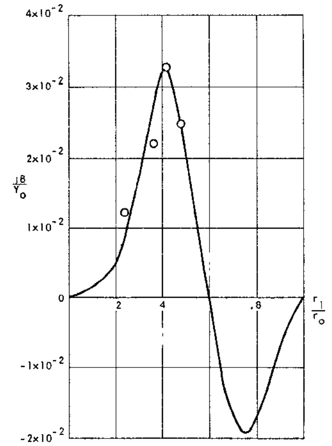

Figure 1 (b) Normalized susceptance for junction of Figure 1 (a) determined from numerical method employing 3 modes in each waveguide Experimental results due to McBride.

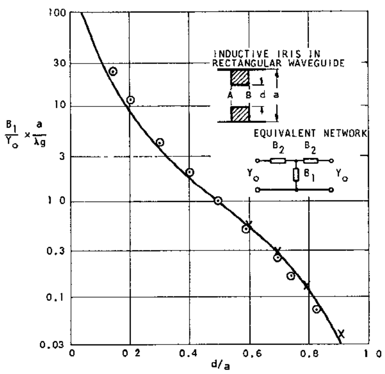

—— NUMERICAL METHOD EMPLOYING 7 MODES IN EACH REGION
⊙⊙⊙ EXPERIMENTAL POINTS FROM T. MORENO "MICROWAVE TRANSMISSION DESIGN DATA"
×-×-× THEORETICAL VALUES FROM N. MARCUVITZ: "WAVEGUIDE HANDBOOK" t/a = 0.035 a/λ_o = 0 8

Figure 2 (a) Shunt susceptance for thick Inductive iris

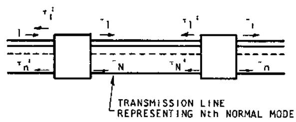

Figure 2 (b)· Schematic equivalent circuit for thick inductive iris

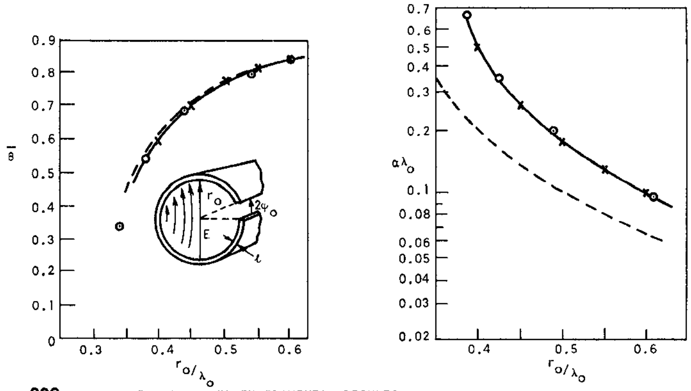

ooo GOLDSTONE AND OLINER EXPERIMENTAL RESULTS

—+— NUMERICAL METHOD WITH 9 MODES INSIDE AND OUTSIDE THE WAVEGUIDE AND 2 MODES INSIDE THE SLOT

--- GOLDSTONE AND OLINER THEORY

$\ell/r_o = 0.143$ $\varphi_o = 15^o$

Figure 3 . $\bar{\beta}$ and $\alpha\lambda_o$ for TE_{11} leaky-waveguide mode.

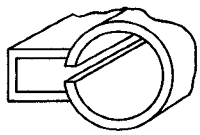

Figure 4

Example of coupled-waveguide structure whose propagation coefficients could be evaluated by means of numerical techniques described herein.